Bismuth-induced synthesis of Au-X (X=Pt, Pd) nanoalloys for electrocatalytic reactions

Nan Wang[a], Wei Zhao[a], Miaolei Zhang[a], Pengfei Cao[a], Shengjun Sun[b], Houyi Ma[a,*], Meng Lin[a,*]

[a] School of Chemistry and Chemical Engineering, Shandong University, Jinan 250100, China.

[b] Shandong Provincial Key Laboratory of Oral Biomedicine, College of Stomatology, Shandong University, Jinan 250021, China.

*Corresponding authors: mlin@sdu.edu.cn (M. Lin); hyma@sdu.edu.cn (H. Ma).

Experimental section

1. Chemical reagents and instrumentals

Tetrachloroauric (III) acid hydrate ($HAuCl_4 \cdot 4H_2O$), potassium nitrate (KNO_3), sodium hydroxide (NaOH) and methanol were purchased from the Sinopharm Chemical Reagent Co., Ltd (Shanghai, China). Chloroplatinic acid hexahydrate ($H_2PtCl_6 \cdot 6H_2O$) and palladium chloride ($PdCl_2$) were obtained from Aladdin Chemistry Co., Ltd (Shanghai, China). Chemical solvents involved in the experiments are all analytically pure and can be used directly without further purification. Field emission scanning electron microscope (FESEM, Hitachi-SU8010) and SEM-EDS mapping analysis were used to investigate the morphology and structure of the catalysts. UV-vis absorption spectra of the prepared nanoalloys were obtained on the Thermo Evolution 220 ultraviolet-visible spectrometer. X-ray diffraction (XRD) patterns were recorded

on a Rigaku D/Max 2200PC diffractometer using a CuKα source (λ = 1.541 Å, with the applied tube voltage and electric current being 40 kV and 20 mA, respectively). High-angle annular dark-field scanning transmission electron microscopy (HAADF-STEM) and elemental mapping images were acquired by energy-dispersive X-ray spectroscopy (EDS) using a JEOL-2100F electron microscope equipped with a STEM unit. CHI 750E workstation (CH Instrument Company, Shanghai, China) was used for electrochemical measurements.

2. Preparation of Au-X nanoalloys

In order to electrochemically deposit Au nanoparticles on the surface of the ITO (1×5 cm) electrode, a series of ITO glasses were immersed in dilute ammonia water (1:3), absolute ethanol and deionized water, sonicated for 5 minutes, respectively. Then the electrode was transferred into an electrolyte which composed of 20.0 mL 0.1 mol L^{-1} KNO_3 solution and 0.4 mL 0.024 mol L^{-1} $HAuCl_4$ for the preparation of Au nanoparticles. At room temperature, the electrodeposition was performed by CV in potential range of 0.2 to -1.0 V for 10 cycles, with a scan rate of 50 mV s^{-1}. After washing thoroughly with deionized water, the obtained Au nanoparticle modified ITO electrode (Au/ITO) was immersed in an electrolyte of potassium nitrate solution (0.1 mol L^{-1}) containing Bi(III) (500 μg/L) to fabricate Au-Bi/ITO with a constant voltage of -1.4 V for 400 s. Subsequently, the Au-Bi/ITO was kept into an aqueous solution of 10 mmol/L Pt(IV) or Pd(II) for 12 hours at room temperature. Compared with Bi, the chemical potential of Pt and Pd is higher, and the Bi atoms on the Au-Bi/ITO can be replaced by Pt or Pd atoms through the GRR, resulting in the formation of Au-X (X=Pt,

Pd) modified ITO electrode.

3. Electrochemical investigation

The Au-X modified ITO glass was used as a working electrode, a saturated calomel electrode (SCE) and a graphite rod electrode were used as reference and counter electrodes, respectively. The electrochemical performances of the Au-X modified electrode in the processes of electrochemical HER and MOR were studied by LSV, CV and chronoamperometry, while a 1.0 mol/L NaOH aqueous solution was used as the supporting electrolyte.

Results and discussion

Several peaks present at values between 46° and 59° in the XRD patterns come from the ITO substrate [1]. For Au-Pt and Au-Pd nanoalloys, a peak near 35° can be attributed to Bi_2Pt [2,3] and BiPd alloys [4]. After electrocatalysis, a new peak emerged 37.4° which can be associated with the (104) plane of metallic Bi [5]. Meanwhile, some sharp peaks between 46° and 59° present in the Au-X patterns. Except for the characteristic peaks of the ITO substrate (black circles), the remaining peaks can be attributed to Bi-X alloys (black arrow). The 2θ=45.16°, 50.98°, 55.40°, 56.37° of Au-Pt nanoalloys correspond to the BiPt alloy [6], and the presence of Bi_2Pd and/or its oxidation stated are observed at 45.27°, 51.02°, 55.35° and 56.47° in the Au-Pd nanoalloy [7]. The structural changes of both nanoalloys can be explained as the partial dissolution, agglomeration and oxidation of nanoparticles during the electrochemical reactions [8-11].

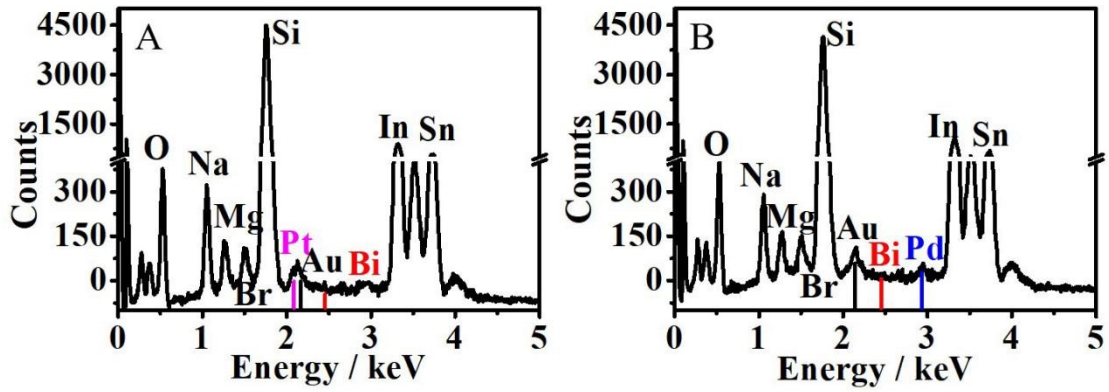

Figure S1. EDS spectra of the Au-Pt/Pd nanoalloys.

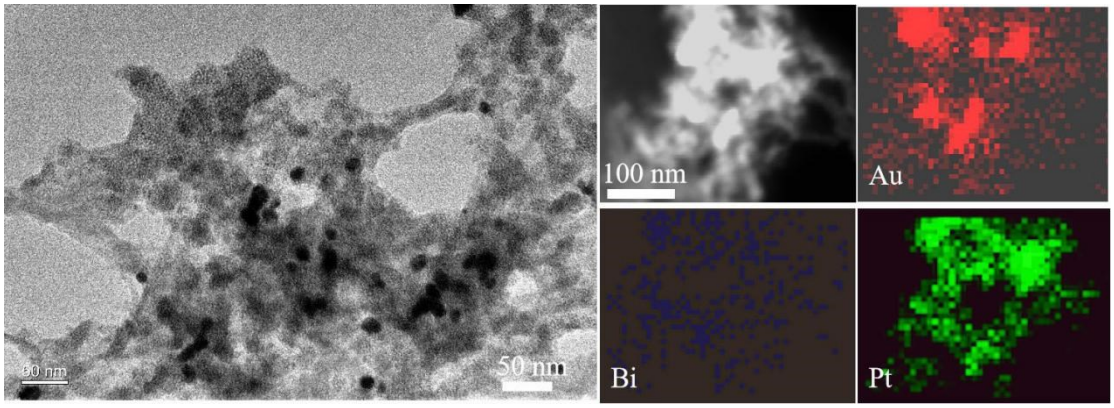

Figure S2. HAADF-STEM image and corresponding elemental mappings of the Au-Pt nanoalloy.

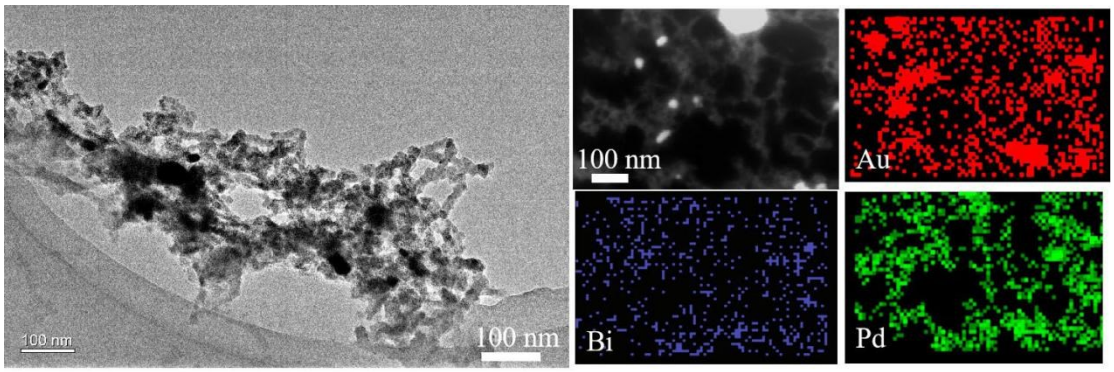

Figure S3. Low-resolution TEM images of the Au-Pd nanoalloy (left image). HAADF-STEM images of the Au-Pd nanoalloy and the corresponding EDS element mapping results (right image).

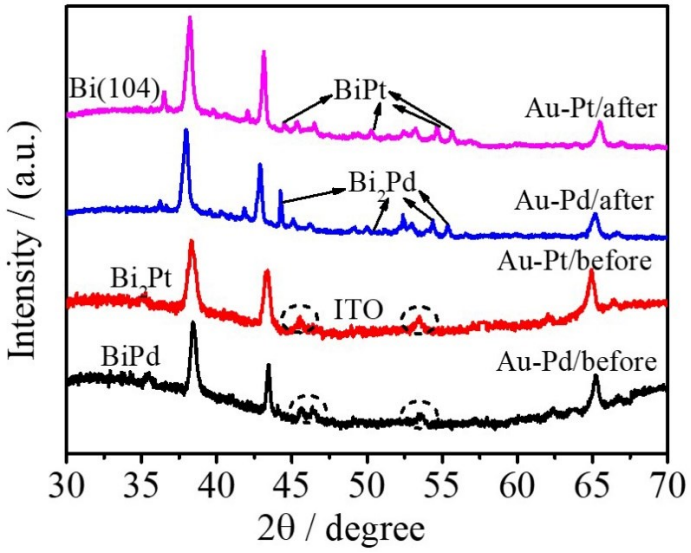

Figure S4. XRD structures of the nanoalloys before and after the electrochemical catalytic reactions.

Table S1. The EDS content distribution of different elements from the Au, Au-Bi, Au-Pt and Au-Pd nanocomposites.

Mass Norm[%] / Element	Au	Bi	Pd	Pt
Au	0.69	-	-	-
Au-Bi	0.67	0.30	-	-
Au-Pt	0.67	-	0.29	-
Au-Pd	0.65	-	-	0.23

Table S2. HER comparative study of recently reported Au/Pt-based metal electrocatalysts

Catalyst	Electrode	Overpotential@ 10 mA cm^{-2} [mV]	Tafel slope [mV dec^{-1}]	Reference
MoS_2/Au	GC	330	57	12
Pt/$Ni(OH)_2$	CC	150		13
$Ni(OH)_2$/PtO_2	Ti	31.4	89	14
Pt/Ni	Ni	75	120	15
PtO_2/Co(OH)F	Ti	160	63	16
Au-Pt nanoalloy	ITO	66	56.53	this work

Table S3. MOR comparative study of recently reported Pd/Pt-based metal electrocatalysts

Catalyst	Electrolyte	Peak current from CV curves [mA cm^{-2}]	Reference
Pd nanoparticles/rGO	0.5 M NaOH + 0.5 M CH_3OH	1.858	17
Pt-Pd/rGO	0.5 M H_2SO_4 + 1.0 M CH_3OH	0.36	18
Pd-Pt/GO	0.5 M $HClO_4$ + 1.0 M CH_3OH	4.35	19
Pd-Pt alloy/rGO	1.0 M NaOH + 0.5 M CH_3OH	2.16	20
Pd nanoparticles/N-doped graphene	1.0 M NaOH + 0.5 M CH_3OH	4.66	21
Au-Pd nanoalloy	1.0 M NaOH + 1.0 M CH_3OH	4.69	this work

References

1. N. Manavizadeh, F. A. Boroumand, E. Asl-Soleimani, F. Raissi, S. Bagherzadeh, A. Khodayari, M. A. Rasouli. Thin Solid Films, 2009, **517**, 2324-2327.

2. F. Dawood, B. M. Leonard, R. E. Schaak. Chem. Mater. 2007, **19**, 4545-4550.

3. L. Sui, W. An, C. K. Rhee, S. H. Hur. J. Electrochem. Sci. Technol., 2020, **11**, 84-91.

4. T. Shen, S. J. Chen. R. Zeng, M. X. Gong, T. H. Zhao, Y. Lu, X. P. Liu, D. D. Xiao, Y. Yang, J. P. Hu, D. L. Wang, L. Xin, and H. D. Abruña. ACS Catal. 2020, **10**, 9977-9985.

5. L. Wang, Z. L. Cui, Z. K. Zhang. Surf. Coat. Tech., 2007, **201**, 5330-5332.

6. M. M. Tusi, N. S. O. Polanco, S. G. da Silva, E. V. Spinacé, A. O. Neto. Electrochem. Commun., 2011, **13**, 143-146.

7. F. Dawood, B. M. Leonard and R. E. Schaak, Chem. Mater. 2007, **19**, 4545-4550.

8. Y. Wang. Nano Energy 2018, **48**, 590-599.

9. A. Zadick, L. Dubau, N. Sergent, G. Berthomé, M. Chatenet. ACS Catal., 2015, **5**, 4819-4824.

10. D. X. Yu, A. J. Wang, L. L. He, J. Yuan, L. Wu, J. R. Chen, J. J. Feng. Electrochim. Acta, 2016, **213**, 565-573.

11. C. H. W. Kelly, T. M. Benedetti, A. Alinezhad, W. Schuhmann, J. J. Gooding, R. D. Tilley. J. Phys. Chem. C 2018, **122**, 21718-21723.

12. J. Kim, S. Byun, A. J. Smith, J. Yu, J. Huang, J. Phys. Chem. Lett. 2013, **4**, 1227-1232

13. H. Yin, S. Zhao, K. Zhao, A. Muqsit, H. Tang, L. Chang, H. Zhao, Y. Gao, Z. Tang, Nat. Commun. 2015, **6**, 6430

14. L. Xie, X. Ren, Q. Liu, G. Cui, R. Ge, A. M. Asiri, X. Sun, Q. Zhang, L. Chen, J. Mater. Chem. A. 2018, **6**, 1967-1970

15. S. Fiameni, I. Herraiz-Cardona, M. Musiani, V. Pérez-Herranz, L. Vázquez-Gómez, E. Verlato, Int. J. Hydrogen Energy 2012, **37**, 10507-10516

16. Z. Wang, Z. Liu, G. Du, A. M. Asiri, L. Wang, X. Li, H. Wang, X. Sun, L. Chen, Q. Zhang, Chem. Commun. 2018, **54**, 810-813

17. H. Yang, L. Geng, Y. Zhang, G. Chang, Z. Zhang, X. Liu, M. Lei, Y. He, Appl. Surf. Sci., 2019, **466**, 385-392

18. G. V. Reddy, P. Raghavendra, P. S. Chandana and L. S. Sarma, RSC Adv., 2015, **5**, 100522-100530

19. M. Khan, A. B. Yousaf, M. Chen, C. Wei, X. Wu, N. Huang, Z. Qi, L. Li, J. Power Sources, 2015, **282**, 520-528

20. K. Wu, Q. Zhang, D. Sun, X. Zhu, Y. Chen, T. Lu, Y. Tang, Int. J. Hydrogen Energy, 2015, **40**, 6530-6537

21. L. Chao, Y. Qin, J. He, D. Ding, F. Chu, Int. J. Hydrogen Energy, 2017, **42**, 15107-15114.